THE JOURNAL OF BIOLOGICAL CHEMISTRY VOL. 290, NO. 14, pp. 9150–9161, April 3, 2015

The BH4 Domain of Anti-apoptotic Bcl-XL, but Not That of the Related Bcl-2, Limits the Voltage-dependent Anion Channel 1 (VDAC1)-mediated Transfer of Pro-apoptotic Ca^{2+} Signals to Mitochondria*

Received for publication, October 29, 2014, and in revised form, February 11, 2015 Published, JBC Papers in Press, February 13, 2015, DOI 10.1074/jbc.M114.622514

Giovanni Monaco[‡1,2,3], Elke Decrock[§1,2], Nir Arbel[¶], Alexander R. van Vliet[‖4], Rita M. La Rovere[‡], Humbert De Smedt[‡], Jan B. Parys[‡], Patrizia Agostinis[‖], Luc Leybaert[§], Varda Shoshan-Barmatz[¶], and Geert Bultynck[‡5]**

*From the [‡]Laboratory of Molecular and Cellular Signaling, Department of Cellular and Molecular Medicine, and [‖]Laboratory of Cell Death Research and Therapy, Department of Cellular and Molecular Medicine, KU Leuven, 3000 Leuven, Belgium, the [§]Physiology Group, Department of Basic Medical Sciences, Faculty of Medicine and Health Sciences, Ghent University, 9000 Ghent, Belgium, the [¶]Department of Life Sciences and the National Institute for Biotechnology in the Negev, Ben-Gurion University of the Negev, Beer-Sheva 84105, Israel, and the **Laboratory of Cellular Physiology, Department of Neuroscience Imaging and Clinical Sciences, Faculty of Pharmacy, "G. D'annunzio" University, 66013 Chieti, Italy*

Background: VDAC1 mediates the transfer of pro-apoptotic Ca^{2+} signals into mitochondria.
Results: The BH4 domain of Bcl-XL, but not that of Bcl-2, targets VDAC1 and suppresses its pro-apoptotic Ca^{2+}-flux properties. N-terminal VDAC1 peptide alleviates this effect of BH4-Bcl-XL.
Conclusion: Bcl-XL via its BH4 domain inhibits VDAC1 activity.
Significance: Bcl-2 and Bcl-XL differ in their BH4 domain biology by regulating ER and mitochondrial Ca^{2+}-transport systems, respectively.

Excessive Ca^{2+} fluxes from the endoplasmic reticulum to the mitochondria result in apoptotic cell death. Bcl-2 and Bcl-XL proteins exert part of their anti-apoptotic function by directly targeting Ca^{2+}-transport systems, like the endoplasmic reticulum-localized inositol 1,4,5-trisphosphate receptors (IP_3Rs) and the voltage-dependent anion channel 1 (VDAC1) at the outer mitochondrial membranes. We previously demonstrated that the Bcl-2 homology 4 (BH4) domain of Bcl-2 protects against Ca^{2+}-dependent apoptosis by binding and inhibiting IP_3Rs, although the BH4 domain of Bcl-XL was protective independently of binding IP_3Rs. Here, we report that in contrast to the BH4 domain of Bcl-2, the BH4 domain of Bcl-XL binds and inhibits VDAC1. In intact cells, delivery of the BH4-Bcl-XL peptide via electroporation limits agonist-induced mitochondrial Ca^{2+} uptake and protects against staurosporine-induced apoptosis, in line with the results obtained with $VDAC1^{-/-}$ cells. Moreover, the delivery of the N-terminal domain of VDAC1 as a synthetic peptide (VDAC1-NP) abolishes the ability of BH4-Bcl-XL to suppress mitochondrial Ca^{2+} uptake and to protect against apoptosis. Importantly, VDAC1-NP did not affect the ability of BH4-Bcl-2 to suppress agonist-induced Ca^{2+} release in the cytosol or to prevent apoptosis, as done instead by an IP_3R-derived peptide. In conclusion, our data indicate that the BH4 domain of Bcl-XL, but not that of Bcl-2, selectively targets VDAC1 and inhibits apoptosis by decreasing VDAC1-mediated Ca^{2+} uptake into the mitochondria.

Intracellular Ca^{2+} signals originating from the endoplasmic reticulum (ER)[6] critically control mitochondrial functions ranging from pro-survival mitochondrial bio-energetics and autophagy to pro-death mitochondrial outer membrane permeabilization (MOMP) and apoptosis (1–3). ER mitochondria Ca^{2+} cross-talk is mainly due to two features as follows: 1) the close proximity between the ER and mitochondria at specific contact sites called mitochondrion-associated ER membranes (MAMs) (4–6); and 2) the high driving force for Ca^{2+} accumu-

* This work was supported in part by Research Foundation-Flanders Grants 6.057.12 (to G. B. and L. L.) and G.0134.09N (to L. L.), Research Council of the KU Leuven Grants STRT1/10/044 and OT/14/101 (to G. B.), Interuniversity Attraction Poles Program, Belgian Science Policy P7/13 (to G. B. and J. B. P.), and Israel Science Foundation Grants 649/09 and 307/13 (to V. S.-B. and N. A.).
[1] Both authors contributed equally to this work.
[2] Supported by postdoctoral fellowships provided by the Research Foundation-Flanders.
[3] To whom correspondence may be addressed: Laboratory of Molecular and Cellular Signaling, Dept. of Cellular and Molecular Medicine, KU Leuven, Campus Gasthuisberg, Herestraat 49, O&N1, bus 802, B-3000 Leuven, Belgium. Tel.: 32-16-33-02-15; E-mail: giovanni.monaco@med.kuleuven.be.
[4] Recipient of a fellowship from Innovation by Science and Technology (IWT) Vlaanderen.
[5] To whom correspondence may be addressed: Laboratory of Molecular and Cellular Signaling, Dept. of Cellular and Molecular Medicine, KU Leuven, Campus Gasthuisberg, Herestraat 49, O&N1, bus 802, B-3000, Leuven, Belgium. Tel.: 32-16-33-02-15; E-mail: geert.bultynck@med.kuleuven.be.

[6] The abbreviations used are: ER, endoplasmic reticulum; BAPTA, 1,2-bis(*o*-aminophenoxy)ethane-*N*,*N*,*N*′,*N*′-tetraacetic acid; BH domain, Bcl-2 homology domain; IDP, IP_3R-derived peptide; IP_3, inositol 1,4,5-trisphosphate; IP_3R, IP_3 receptor; MAM, mitochondrion-associated ER membranes HBSS, Hanks' balanced salt solution; MEF, mouse embryonic fibroblast; MOM, mitochondrial outer membrane; MOMP, mitochondrial outer membrane permeabilization; STS, staurosporine; VDAC, voltage-dependent anion channel; VDAC1-NP, VDAC1 N-terminal peptide; OMM, outer mitochondrial membrane; BisTris, 2-[bis(2-hydroxyethyl)amino]-2-(hydroxymethyl)propane-1,3-diol.

lation into the matrix of the mitochondria, due to an existing membrane potential, usually between −150 and −180 mV, across the inner mitochondrial membrane (7). MAMs are hotspots for the Ca^{2+} transfer mediated by ER and mitochondrial Ca^{2+}-transport mechanisms that are physically linked. Inositol 1,4,5-trisphosphate (IP_3) receptors (IP_3Rs), ER-resident intracellular Ca^{2+}-release channels, are indirectly linked to the Ca^{2+}-permeable voltage-dependent anion channels (VDACs) (8, 9). Further studies revealed that particular isoforms may be preferentially located in the MAMs. For instance, in HeLa cells IP_3R3 and VDAC1 have been specifically involved in mediating the transfer of pro-apoptotic Ca^{2+} signals from the ER into the mitochondria (10, 11).

Given the central role of the IP_3R and VDAC1 in apoptosis (12, 13), it is not surprising that anti- and pro-apoptotic proteins target these channels, thereby controlling the cellular sensitivity to Ca^{2+}-dependent apoptosis. In particular, different anti-apoptotic members of the Bcl-2 protein family, including Bcl-2, Bcl-XL, and Mcl-1, have attributed important roles in regulating IP_3R and VDAC1 channel activities, thereby exerting part of their anti-apoptotic function via the control of Ca^{2+} fluxes across ER and mitochondrial membranes (14–17). Furthermore, selective roles for distinct anti-apoptotic Bcl-2 family members are emerging. Bcl-2 mainly suppresses pro-apoptotic Ca^{2+} transients by dampening Ca^{2+} flux through IP_3R channels (18), although Bcl-XL promotes pro-survival Ca^{2+} oscillations by sensitizing IP_3Rs to low levels of IP_3 signaling (19). These distinct effects of Bcl-2 and Bcl-XL on IP_3R function reflect differences in the molecular determinants underlying their interaction with the IP_3R. Bcl-2 through its BH4 domain targets a site located in the center of the modulatory and regulatory domain of the IP_3R, although Bcl-XL, through a yet unidentified domain, preferentially targets the 6th transmembrane domain located in the proximity of the C-terminal part of the IP_3R's Ca^{2+} channel pore (20).

We recently found a critical and conserved difference between the BH4 domain of Bcl-2 (Lys-17) and Bcl-XL (Asp-11), being responsible for the privileged binding and inhibition of IP_3R channels by BH4-Bcl-2 but not by BH4-Bcl-XL (21). Moreover, although both BH4-Bcl-2 and BH4-Bcl-XL were able to protect against apoptosis upstream of MOMP, only BH4-Bcl-2-mediated protection was abolished by the co-addition of a peptide corresponding to the Bcl-2-binding site on IP_3Rs (IP_3R-derived peptide; IDP). In addition, the co-administration of both BH4-Bcl-2 and BH4-Bcl-XL peptides did not provide any additive protective effect against apoptosis, and neither BH4-Bcl-2 nor BH4-Bcl-XL protected against cell death induced by procaspase-activating compound 1, a post-MOMP caspase (cysteine-dependent aspartate-specific protease) activator (21, 22). Hence, we hypothesized that the protective effect of BH4-Bcl-XL was due to its action on a target downstream of IP_3R signaling but upstream of caspases, *e.g.* at the cross-road between ER and mitochondria. Considering the preferential distribution of Bcl-XL to the OMM (23, 24), we therefore anticipated the possible involvement of a mitochondrial target. In this respect, earlier studies (25) showed that the BH4 domain of Bcl-XL was more potent than the one of Bcl-2 in suppressing VDAC1-mediated mitochondrial swelling. Later studies also revealed that Bcl-2 and Bcl-XL proteins directly bind to VDAC1 and modulate its conductance, with the VDAC1 N-terminal region being an important region for its function (26–30).

TABLE 1
List of the different peptide sequences used in this study for molecular and functional analyses

Peptide name	Amino acid sequence
BH4-Bcl-2	RTGYDNREIVMKYIHYKLSQRGYEW
BH4-Bcl-XL	MSQSNRELVVDFLSYKLSQKGYSW
Biotin-BH4-Bcl-2	Biotin-RTGYDNREIVMKYIHYKLSQRGYEW
Biotin-BH4-Bcl-XL	Biotin-MSQSNRELVVDFLSYKLSQKGYSW
Biotin-BH4-Bcl-2 scramble	Biotin-WYEKQRSLHGIMYYVIEDRNTKGYR
Biotin-BH4-Bcl-XL scramble	Biotin-WYSKQRSLSGLVMYVLEDKNSQFS
IDP	NVYTEIKCNSLLPLDDIVRV
VDAC1-NP	MAVPPTYADLGKSARDVFTKGYGFGL
VDAC1-NP scramble	DKVPAAKTYLMVRFSDTGGPLYAFGG

Driven by these previous studies and observations, we hypothesized that the anti-apoptotic effect of the BH4 domain of Bcl-XL could be due to its targeting of VDAC1 and inhibition of VDAC1-mediated Ca^{2+} transfer into the mitochondria. To test this assumption, we first re-examined the role of VDAC1 as a mitochondrial Ca^{2+} entry mechanism and simultaneously profiled the molecular interaction of VDAC1 with both Bcl-2 and Bcl-XL. We compared the alleged ability of Bcl-2 and Bcl-XL BH4 peptides to bind VDAC1, to control its single channel activity, and to protect against Ca^{2+}-mediated apoptosis. Our results propose a novel role for the BH4 domain of Bcl-XL in apoptosis and in mitochondrial Ca^{2+} entry by controlling VDAC1 channel conductance, while the BH4 domain of Bcl-2 would mainly act at the level of the IP_3R channels.

EXPERIMENTAL PROCEDURES

Cell Culture and Peptides—Both wild-type (WT) and VDAC1 knock-out ($VDAC1^{-/-}$) mouse embryo fibroblast cells (MEFs) were kindly provided by Dr. W. J. Craigen, Baylor College of Medicine, Houston, TX (31). MEFs were maintained at 37 °C and 5% CO_2 in DMEM medium (Life Technologies, Inc.) supplemented with 10% fetal bovine serum (Sigma), 2 mM L-glutamine (GlutaMAX, Life Technologies), 1 mM pyruvate, 1% penicillin/streptomycin. Rat C6 glioma cells and COS-1 cells were cultured as described previously (21). Peptides used in this study were obtained from Thermo Electron (Germany) or from Lifetein when biotinylation was necessary. All peptides were more than 80% pure, and their identity was confirmed via mass spectrometry. Their respective amino acidic sequences are given in Table 1.

SDS-PAGE, Western Blotting, and Antibodies—COS-1 and MEFs were lysed in a lysis buffer containing 10 mM Hepes, pH 7.5, 0.25% Nonidet P-40, 142 mM KCl, 5 mM $MgCl_2$, 2 mM EDTA, 1 mM EGTA and containing protease inhibitor mixture (Roche Applied Science). The Bradford assay (Sigma) was used to determine sample protein concentrations relative to the standard curve of bovine serum albumin (BSA). Samples for SDS-PAGE were prepared by adding NuPAGE LDS Sample Buffer (Life Technologies, 1.6-fold final concentration) and 5 min of incubation at 70 °C. Proteins samples (10–20 μg) were

separated by NuPAGE 4–12% or 10% BisTris SDS-polyacrylamide gels using MOPS/SDS-running buffer (Life Technologies). When needed, gels were stained with GelCode™ blue stain reagent (Pierce) following the manufacturer's recommendations. Alternatively, gels were transferred onto a polyvinylidene fluoride (PVDF) membrane. After blocking with TBS (50 mM Tris, 150 mM NaCl, pH 7.5) containing 0.1% Tween and 5% nonfat dry milk, membranes were incubated with the primary antibody overnight as appropriate, *i.e.* anti-FLAG M2 (clone M2, Sigma, 1:10,000); anti-VDAC1 (clone D73D12, Cell Signaling, 1:1000, or polyclonal anti-C-terminal, Antibodies Online, 1:1000); anti-β-actin (clone AC-15, Sigma, 1:20,000); Rbt475 (in-house developed pan-IP_3R antibody (32), 1:2000); anti-calnexin (Enzo Life Science, 1:1000); anti-Bcl-XL (clone YTH-2H12, Trevigen, 1:1000); anti-Bcl-2 (clone C-2, Santa Cruz Biotechnology, 1:1000); and anti-cytochrome *c* (BD Biosciences, 1:1000). Next, membranes were incubated for 1 h with a secondary horseradish peroxidase (HRP)-conjugated antibody (Cell Signaling Technology, dilution 1:2000 in 0.1% Tween/TBS). Immunoreactive proteins were detected using the ECL Western blotting Substrate (Thermo Fisher Scientific, Belgium). The resulting bands were quantified using ImageJ software (rsbweb.nih.gov).

Isolation of MAMs—Isolations of MAMs were performed by an adaptation of the protocol described in Ref. 33. Approximately 100×10^6 MEFs were collected after culture and homogenized in isolation buffer 1 (225 mM mannitol, 75 mM sucrose, 0.1 mM EGTA, and 30 mM Tris-HCl, pH 7.4). The homogenate was spun at $600 \times g$ for 10 min to remove entire cells and nuclei; the supernatant was recovered and further centrifuged for 10 min at $7000 \times g$. Supernatant was removed, and the pellet was washed in isolation buffer 1 before being centrifuged at $10,000 \times g$ for 10 min. Pellet was then resuspended in isolation buffer 2 (225 mM mannitol, 75 mM sucrose, and 30 mM Tris-HCl, pH 7.4). The homogenate was purified by centrifugation at $95,000 \times g$ for 30 min on a Percoll™ density gradient in isolation buffer 1 (a 15% Percoll gradient on a 30% layer). The low density bands (denoted as MAMs) and the high density bands (denoted as pure mitochondria) were collected. The obtained mitochondrial layer was washed free of Percoll and resuspended in isolation buffer 2. MAMs were centrifuged for 10 min at $7000 \times g$ three times to remove mitochondrial contamination and finally centrifuged at $100000 \times g$ for 1 h. The MAM fraction pellet was collected and concentrated using Pierce Protein Concentrators, 9K MWCO (Thermo Fisher Scientific Inc.) before Western blotting.

FLAG Immunoprecipitation Assay—For immunoprecipitation, 300 μg of protein lysate from COS-1 cells overexpressing Bcl-2 or Bcl-XL in the 3×FLAG pCMV-24 vector (Sigma) was added to 30 μl of anti-FLAG M2-agarose affinity gel (Sigma) previously washed according to the manufacturer's protocol. Successively, the samples were incubated in lysis buffer (see lysis buffer under "SDS-PAGE, Western Blotting, and Antibodies") at 4 °C. After 2 h, the beads were washed twice in spin columns (Pierce) with washing buffer (150 mM NaCl, 1.0% Nonidet P-40, 0.5% sodium deoxycholate, 0.1% SDS, 50 mM Tris, pH 8.0). Protein complexes containing FLAG fusion proteins were eluted by incubating the beads for 30 min with 35 μg of 3×FLAG peptide (Sigma, final concentration 150 ng/μl), and the eluate was subjected to Western blot analysis.

Biotin Pulldowns—Neutravidin-agarose resin (Pierce) (25 μl) was added to the tested sample and washed according to the manufacturer's guidelines. Next, 30 μg of each biotinylated peptide was bound to the resin in interaction buffer (50 mM Tris-HCl, pH 7.5, 200 mM NaCl; 0.1% Nonidet P-40, protease inhibitor mixture (Pierce)) that contains 500 μg of COS-1 total cell lysate expressing endogenous VDAC1 or an ectopic version of VDAC1 N-terminally truncated (Δ(1–26)-VDAC1, pcDNA4/TO vector (28)). After overnight mixing, beads were washed three times with interaction buffer in spin columns before proceeding with SDS-PAGE and Western blotting.

VDAC1 Single Channel Current Recordings—VDAC1 purified from rat liver mitochondria was solubilized with *N*,*N*-dimethyldodecylamine-*N*-oxide and purified using hydroxyapatite resin, as described previously (26). Purified VDAC1 was used for channel reconstitution into a planar lipid bilayer prepared from soybean asolectin dissolved in *n*-decane (50 mg/ml). Purified VDAC1 was added to the *cis* chamber containing 1 M NaCl and 10 mM Hepes, pH 7.4. After one or more channels were inserted into the planar lipid bilayer, currents were recorded by voltage clamping using a Bilayer ClampBC-525B amplifier (Warner Instruments). Current was measured with respect to the *trans* side of the membrane (ground). The current was digitized online using a Digidata 1200 interface board and pCLAMP10.2 software (Axon Instruments). Three independent recordings have been collected.

Electroporation Loading—In situ electroporation of adherent C6 cell monolayer cultures was performed, as described previously (21, 34), following a procedure optimized for cell death studies (35). In brief, C6 cell monolayers were placed 400 μm underneath a two-wire Pt-Ir electrode on the microscopic stage and electroporated in the presence of solution (10 μl) containing peptides (20 μM) or vehicle (DMSO, final 0.2%) dissolved in electroporation buffer (4.02 mM KH_2PO_4, 10.8mM K_2HPO_4, 1.0 mM $MgCl_2$, 300 mM sorbitol, 2.0mM Hepes, pH 7.4) (10 μl). Electroporation was done with 50 kHz bipolar pulses applied as trains of 10 pulses of 2 ms duration each and repeated 15 times. Cells were electroporated in the presence of 100 μM dextran Texas red (Life Technologies) to define the electroporated zone. After electroporation, cells were thoroughly washed with HBSS/Hepes and left for 5 min to recover before proceeding with Ca^{2+} imaging or apoptosis assay.

Mitochondrial and Cytosolic Ca^{2+} Measurements—Changes in $[Ca^{2+}]_{mit}$ and $[Ca^{2+}]_{cyt}$ in MEFs or C6 cells were triggered by 200 or 2 μM ATP, respectively, and monitored as described previously (34, 36). Briefly, C6 or MEFs cells were seeded on 18-mm diameter glass coverslips, and experiments were performed the next day after loading cells for 30 min with 10 μM Fluo3-AM (cytosol) or 5 μM Rhod-FF-AM (mitochondria). Subsequently, cells were subjected to de-esterification over 15 min and loaded with 100 μM dextran Texas red and 20 μM BH4 peptides using the *in situ* electroporation technique as described above. Ca^{2+} imaging was performed with an inverted Nikon Eclipse TE300 fluorescence microscope (Nikon, Belgium) equipped with a ×40 oil immersion objective (Plan Fluor, NA 1.3) and an EM-CCD camera (QuantEM 512SC, Photomet-

rics). Cells were perfused for 1 min with HBSS-Hepes followed by 4 min (MEFs) or 9 min (C6 cells) with ATP (Sigma) in HBSS-Hepes. Alternatively, cells were kept in 1,2-bis(*o*-aminophenoxy)ethane-*N,N,N′,N′*-tetraacetic acid (BAPTA, 3 mM; Sigma) to chelate extracellular Ca^{2+} before (1 min) and during the ATP addition images (1/s) were generated with custom-developed software written in Microsoft Visual C^{++} 6.0. Fluorescence-intensity changes in all cells/mitochondria were analyzed. For each individual trace, the relative change of fluorescence ($\Delta F/F$) was calculated. $\Delta F/F$ equals $F_t - F_0/F_0$, with F_0 denoting the fluorescence before stimulation with ATP and F_t, the fluorescence at different time points after ATP stimulation. Subsequently, relative $[Ca^{2+}]_{cyt}$ or $[Ca^{2+}]_{mit}$ changes were quantified as the area under the curve of the various Ca^{2+} traces. Data were normalized to the control condition (DMSO, 0.2%), which was set as 100%. A minimum of three dishes has been used for each condition.

Apoptosis Assay—MEFs and C6 cells were kept in 200 μl of culture medium containing 2 μM staurosporine (STS) (Sigma). Six hours later, cultures were stained with 10 μM of the CaspACE^{TM} FITC-VAD-FMK *In situ* Marker (Promega Benelux, The Netherlands) in HBSS-Hepes for 40 min at 37 °C. After fixing the cells with 4% paraformaldehyde for 25 min at room temperature, nuclei were additionally stained for 5 min with 1 μg/ml DAPI (Sigma) in PBS supplemented with Ca^{2+} and Mg^{2+} (Life Technologies). Cells were then mounted with Vectashield fluorescent mounting medium (Labconsult, Belgium) on glass slides. Apoptosis in MEFs in the presence or absence of STS was quantified by taking five images in each culture using a Nikon TE300 epifluorescence microscope equipped with a ×10 objective (Plan APO, NA 0.45; Nikon) and a Nikon DS-Ri1 camera (Nikon, Belgium). The number of caspase-positive cells was counted in each image and expressed relative to the number of nuclei present. Analysis was carried out by making use of custom-developed counting software. The STS-induced apoptosis in C6 cultures was quantified as for MEFs but expressed relative to the STS-induced apoptosis outside the electroporated area.

Data and Statistical Analysis—Data are expressed as means ± S.E., except for Western blot (mean ± S.D.). Statistically significant differences were considered at $p < 0.05$ (single symbols) or $p < 0.01$ (double symbols) after using a two-tailed paired Student's *t* test (Excel Microsoft Office) or one-way analysis of variance and a Bonferroni post-test using Origin7.0.

RESULTS

VDAC1 Is Essential for Transferring Ca^{2+} Signals to the Mitochondria and Determines the Apoptotic Sensitivity toward Staurosporine—In an initial set of experiments, we established the contribution of VDAC1 in the transfer of Ca^{2+} signals from the ER to the mitochondria. Therefore, we compared mitochondrial Ca^{2+} signals in response to extracellular agonists between WT and VDAC1$^{-/-}$ MEFs loaded with Rhod-FF-AM, a mitochondrial Ca^{2+} indicator. The lack of VDAC1 expression in the VDAC1$^{-/-}$ MEFs was confirmed by Western blot analysis (Fig. 1*A*). Extracellular ATP was used to trigger intracellular IP_3 production that subsequently induces Ca^{2+} release from the ER (37). In WT MEFs, ATP (200 μM) caused a transient increase in the mitochondrial Ca^{2+} signal (Fig. 1, *B* and *C*). In VDAC1$^{-/-}$ MEFs, the ATP-triggered increase in mitochondrial Ca^{2+} was severely compromised. Quantitative analysis of five independent experiments showed that cells lacking VDAC1 displayed a more than 95% reduction in the maximal amplitude of the ATP-triggered mitochondrial Ca^{2+} transient (Fig. 1*C*). To verify that the mitochondrial Ca^{2+} handling was specifically targeted, we also compared the cytosolic Ca^{2+} signals between Fluo3-AM-loaded WT and VDAC1$^{-/-}$ MEFs in response to ATP (Fig. 1, *D* and *E*). These data show that both cell types exhibit an increase in cytosolic Ca^{2+} in response to ATP, indicating that the Ca^{2+} release from the ER is not compromised in VDAC1$^{-/-}$ MEFs. Moreover, the VDAC1$^{-/-}$ MEFs show a relatively higher ($p = 0.11$) rise of Ca^{2+} levels in their cytosol after ATP stimulation. This finding is in accordance with the decreased mitochondrial Ca^{2+} uptake (Fig. 1, *B* and *C*).

Next, we examined the influence of VDAC1 knock-out on the cellular sensitivity to STS, a known apoptosis inducer that also leads to mobilization of intracellular Ca^{2+} (38). Therefore, we exposed WT and VDAC1$^{-/-}$ MEFs to staurosporine (1 μM; 6 h) and quantified their apoptotic response by counting the number of apoptotic cells in the population using a fluorescent caspase marker (Fig. 1*F*). We found that VDAC1$^{-/-}$ MEFs were considerably more resistant toward STS-induced apoptosis than their WT counterparts. These results correlate with previous data showing that VDAC1 is required for mitochondrial Ca^{2+} loading in response to extracellular agonists and that it dictates the sensitivity toward apoptotic stimuli (11, 39).

BH4 Domain of Bcl-XL, but Not That of Bcl-2, Specifically Interacts with VDAC1—Because Bcl-2 and Bcl-XL modulation of the ER-mitochondrial Ca^{2+} transfer is likely occurring at the close contact sites between these two organelles (11), we therefore assessed whether VDAC1, IP_3Rs, Bcl-2, and Bcl-XL localize at the MAMs as anticipated or indicated by previous studies (1, 40, 41). The immunoblotting results (Fig. 2*A*) confirmed the presence of these proteins in our MAM preparations, which appeared pure considering that cytochrome *c* and calnexin were exclusively enriched in the mitochondrial and MAM fraction, respectively. Following up on the previously reported binding of Bcl-2 and Bcl-XL with VDAC1 (26, 27), we also compared their relative strengths of interaction by performing affinity pulldowns with COS-1 cells ectopically expressing 3×FLAG-tagged Bcl-2 and Bcl-XL (Fig. 2*B*) and containing high endogenous levels of VDAC1. We found that both proteins bind to VDAC1, although 3×FLAG-Bcl-XL tended to exhibit a higher binding capacity than 3×FLAG-Bcl-2 (Fig. 2*C*, $p = 0.08$ in a two-tailed *t* test). Next, we examined whether the isolated BH4 domains of Bcl-2 and Bcl-XL differ in their VDAC1-binding properties. To investigate this, we performed affinity pulldowns with COS-1 cells using biotinylated BH4-Bcl-2 or BH-Bcl-XL peptides conjugated to NeutrAvidin beads. These experiments showed that biotin-BH4-Bcl-XL strongly interacts with VDAC1 (Fig. 2*D*, *upper blot*), although this is not the case for biotin-BH4-Bcl-2. We also performed affinity pulldown assays using an ectopically expressed version of VDAC1 lacking its first 26 amino acids (Δ(1–26)-VDAC1), because the VDAC1 N-terminal region has been previously proposed as a target for Bcl-2 and Bcl-XL (26, 27). However, in these experi-

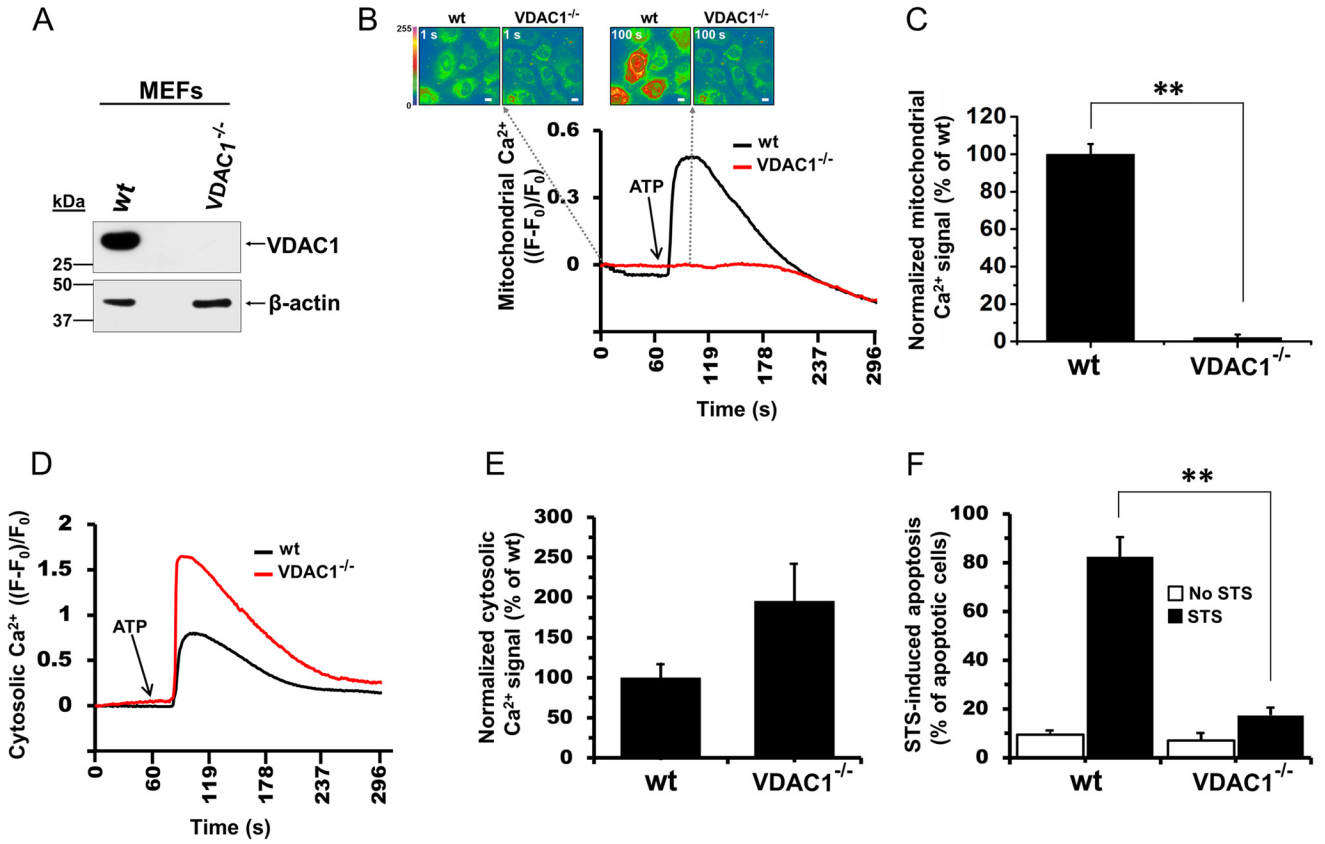

FIGURE 1. **VDAC1$^{-/-}$ MEFs show impaired mitochondrial Ca^{2+} loading and a manifest reduction of apoptotic response to staurosporine.** *A,* MEF WT or VDAC1$^{-/-}$ cells were lysed and subjected to immunoblotting using an anti-VDAC1 antibody (*upper panel*) and using β-actin as loading control (*lower panel,* anti-β-actin). *B, top,* illustrative pseudo-colored images of MEF cells loaded with Rhod-FF-AM before (*left panels*; 1 s) and after (*right panels*; 100 s) exposure to ATP (200 μM). ATP was administered at 60 s. The *scale bar* measures 10 μm. *B, bottom,* representative Ca^{2+} traces obtained from WT or VDAC1$^{-/-}$ MEFs loaded with Rhod-FF-AM. The relative changes in fluorescence with respect to baseline ($F - F_0/F_0$) reflect the changes in mitochondrial Ca^{2+} level in response to ATP (*arrow*). *C,* quantitative analysis of the area under the curve obtained from at least five independent experiments. *D,* representative increases in Fluo3 fluorescence ($F - F_0/F_0$) of ATP-stimulated (200 μM, *arrow*) WT or VDAC1$^{-/-}$ MEFs. Increases in fluorescence normalized to baseline reflect the extent of the cytosolic Ca^{2+} transients. *E,* quantitative analysis of the area under the curve obtained from at least three independent experiments. Data were normalized to the WT condition of MEFs, which was set as 100% for each experiment, and were plotted as means ± S.E. *F,* quantification of the percentage of MEFs (WT and VDAC1$^{-/-}$) stained positive for active caspases in response to STS (1 μM, 6 h). Data points represent mean ± S.E. Statistically significant differences between the two examined cell lines are indicated by $p < 0.01$ (**).

ments, Δ(1–26)-VDAC1, in contrast to full-length VDAC1, displayed a high level of background binding to the beads due to nonspecific interactions, thereby hampering the evaluation of the specific interactions between the biotin-BH4 domains and Δ(1–26)-VDAC1 (data not shown).

BH4-Bcl-XL but Not BH4-Bcl-2 Decreases VDAC1 Single Channel Conductance—Next, we examined whether the differential interaction of BH4-Bcl-2 and BH4-Bcl-XL with VDAC1 leads to differences in VDAC1 channel properties. Purified mitochondrial VDAC1 was reconstituted into a planar lipid bilayer, and channel activity was studied under voltage clamp conditions. The current produced in response to voltage steps from a holding potential of 0 to −10 or to −60 mV was recorded before and 10–15 min after the addition of BH4-Bcl-XL or BH4-Bcl-2 peptides (6 μM; Fig. 3, *A* and *B*). At −10 mV, the channel conductance was reduced by application of the BH4-Bcl-XL peptide, with the channel being stabilized at a low conducting state, whereas BH4-Bcl-2 peptide had no effect (Fig. 3*A*). When the channel activity was monitored at −60 mV, the typical effect of high voltage on VDAC1 conductance is clearly visible, with the channel fluctuating between sub-states (Fig. 3*B*). At this voltage step, the BH4-Bcl-XL peptide, but not the BH4-Bcl-2 peptide, eliminated the channel fluctuations between subconducting states, stabilizing the channel in a single subconducting state (Fig. 3*B*). Moreover, the BH4-Bcl-XL peptide reduced VDAC1 channel conductance at voltages between −50 and +30 mV (Fig. 3*C*). At higher negative or positive voltages, rather an increase in the channel conductance was observed. The increase in the relative conductance of the channel observed at high voltages can be explained by the peptide eliminating channel fluctuations to sub-states with low conductance, thus the average conductance is increased. In contrast, the BH4-Bcl-2 peptide had, at all voltages tested, no effect on the conductance of bilayer-reconstituted VDAC1 (Fig. 3*D*). These results indicate that BH4-Bcl-XL, but not BH4-Bcl-2, inhibits VDAC1 channel conductance.

BH4-Bcl-XL and BH4-Bcl-2 Affect Mitochondrial Ca^{2+} Transfer and Apoptosis via Their Activity on VDAC1 and on IP_3Rs, Respectively—To estimate the physiological relevance of the divergent biophysical regulation of VDAC1 by BH4-Bcl-2 and BH4-Bcl-XL, we exploited a C6 glioma cell model previously optimized for peptide electroporation and for measuring Ca^{2+} signaling and apoptosis events (21, 34). As expected, electroporation of BH4-Bcl-2 or BH4-Bcl-XL peptides (20 μM) into

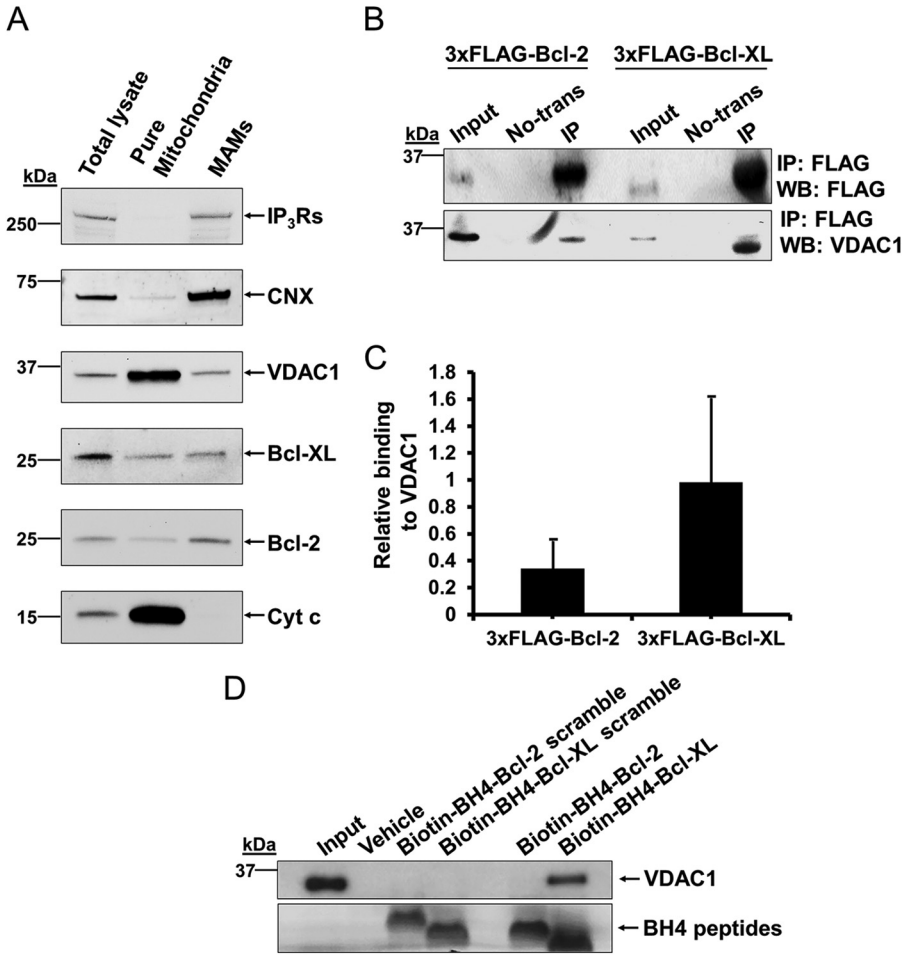

FIGURE 2. **Isolated BH4 domain of Bcl-2 and Bcl-XL differentially interact with VDAC1.** *A,* representative immunoblotting showing the presence of VDAC1, IP_3Rs, Bcl-2, and Bcl-XL in the MAMs of MEFs. Twenty micrograms of proteins from each fraction were loaded. Different portions of the same blot have been used for each protein detection. Calnexin (*CNX*) and cytochrome *c* (*Cyt c*) were used as specific MAMs and mitochondrial markers, respectively. Three independent isolations were performed yielding similar results. *B,* representative Western blots showing the immunoprecipitation (*IP*) of 3×FLAG-Bcl-2 or 3×FLAG-Bcl-XL ectopically expressed in COS-1 cells (*upper blot*, HRP-conjugated anti-FLAG antibody) and the respective co-immunoprecipitation (*Co-IP*) of endogenous VDAC1 (*lower blot*, anti-VDAC1). *WB,* Western blot. *C,* immunoreactive bands of at least five independent experiments were quantified using ImageJ software. Values were normalized considering both the retained amount of 3×FLAG-tagged proteins and the basal expression of VDAC1 (*Input*). Data points represent mean ± S.D. *D,* pulldown experiment showing the binding of endogenous VDAC1 from COS-1 cells (same antibody as in *B*) to different biotinylated peptides (40 μM) encompassing the BH4 domains of Bcl-2 or Bcl-XL (Biotin-BH4-Bcl-2/Bcl-XL) or their scrambled versions (Biotin-BH4-Bcl-2/Bcl-XL scramble). The results of this assay were consistent across three independent experiments. The presence of the biotinylated peptides in each given sample was validated by Coomassie Blue staining (*lower panel*).

the cells suppressed ATP-induced mitochondrial Ca^{2+} transients (Fig. 4, *A–C*, see also Fig. 1*H* of Ref. 21).

Along with the BH4-Bcl-2 or BH4-Bcl-XL peptide, cells were co-electroporated either with the IP_3R-derived peptide (IDP) or the VDAC1 N-terminal peptide (VDAC1-NP). The former corresponds to the Bcl-2-binding site on IP_3Rs (21, 42, 43), and the latter mimics the N terminus of VDAC1, a presumed target of Bcl-XL (26, 27). BH4-Bcl-2-mediated inhibition of mitochondrial Ca^{2+} transients was completely reversed by co-loading IDP but was not altered by the presence of VDAC1-NP (Fig. 4, *B* and *C*). In contrast, BH4-Bcl-XL-mediated inhibition of mitochondrial Ca^{2+} transients could be reversed by co-loading VDAC1-NP but not IDP (Fig. 4, *B* and *C*). Similar results were obtained by stimulating the cells with ATP in the presence of extracellular BAPTA to chelate extracellular Ca^{2+} (Fig. 4*D*), indicating that Ca^{2+} influx did not impinge on the ER-mitochondrial Ca^{2+} transfer.

In a final step, we examined the relevance of the above results in the context of Ca^{2+}-mediated apoptosis by exposing C6 cells to STS (Fig. 4*E*). Both BH4-Bcl-2 and BH4-Bcl-XL protected against STS-induced apoptosis, but BH4-Bcl-2 was significantly more protective than BH4-Bcl-XL, as observed previously (21). The co-loading of VDAC1-NP alleviated BH4-Bcl-XL-mediated protection against apoptosis but not that of BH4-Bcl-2 (Fig. 4*E*). In contrast, we previously reported that IDP co-electroporation exclusively counteracted BH4-Bcl-2-mediated protection against apoptosis (21). Altogether, these data indicate a selective action in both Ca^{2+} signaling and Ca^{2+}-dependent apoptosis of the BH4 domain of Bcl-2 and Bcl-XL by their role on IP_3Rs and VDAC1, respectively.

DISCUSSION

IP_3Rs and VDAC1 channels, intracellular Ca^{2+}-transport systems at the interface between ER and mitochondria, play a

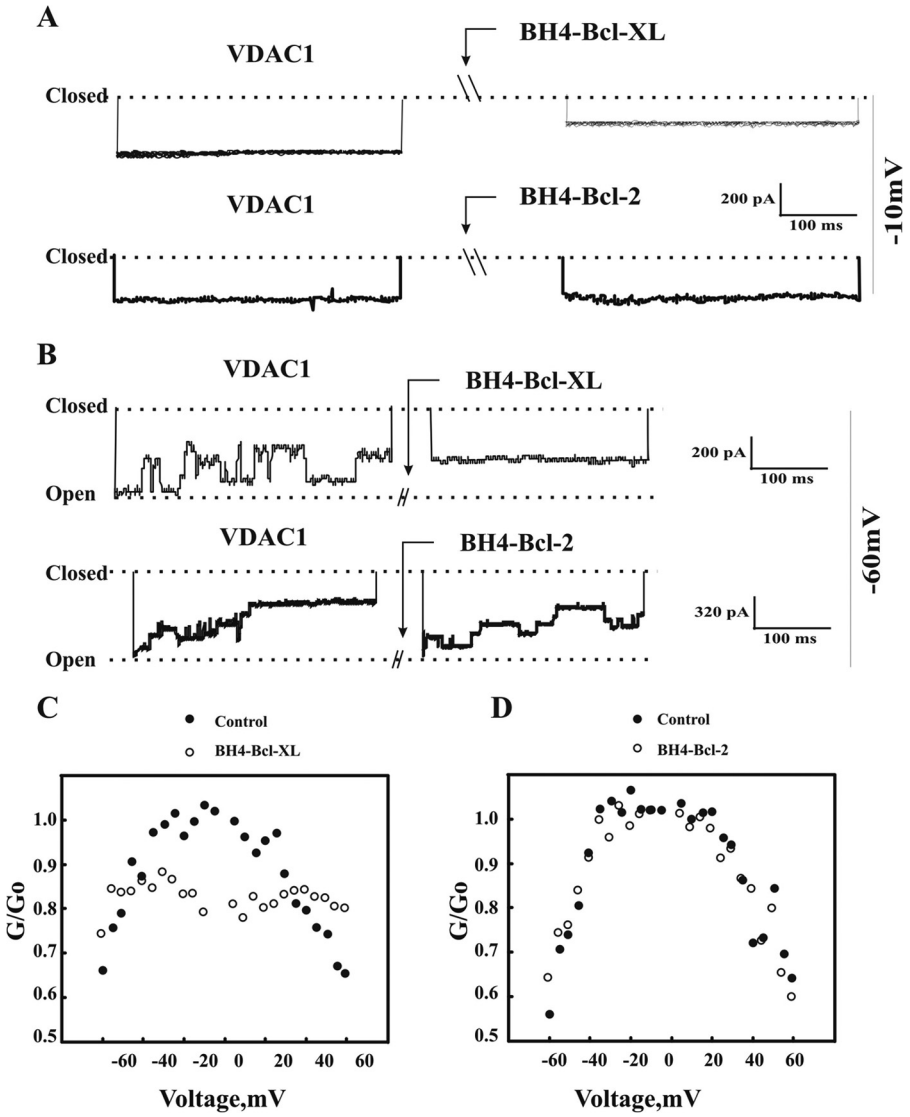

FIGURE 3. **Differential effect of BH4-Bcl-XL- and BH4-Bcl-2-based peptides on the conductance of bilayer-reconstituted VDAC1.** *A,* VDAC1 was reconstituted into a planar lipid bilayer, and current in response to a voltage step from 0 to −10 mV was recorded before and 10–15 min after the addition of BH4-Bcl-XL or BH4-Bcl-2 peptide (6 μM). *B,* VDAC1-mediated currents at −60 mV, before and after the addition of BH4-Bcl-XL or BH4-Bcl-2 peptide. The *dashed lines* indicate the zero and the maximal current levels. *C* and *D* show the multichannel recordings as a function of the voltage (4 s at each voltage), and the average steady-state conductance of VDAC1 before (●) and 10 min after (○) the addition of BH4-Bcl-XL peptide (*C*) or BH4-Bcl-2-peptide (*D*). Relative conductance was determined as the ratio of the conductance at a given voltage (*G*) to the maximal conductance (*Go*). The results are representative of three similar independent experiments.

critical role in determining cell fate. VDAC1 channels are important players in cell survival *versus* cell death processes by mediating Ca^{2+} transfer across the OMM. Previous work revealed a unique role of the BH4 domain of Bcl-2, but not the BH4 domain of Bcl-XL, to suppress "toxic" Ca^{2+} flux originating from the ER, by targeting and inhibiting IP_3R channels (21). We now report that the BH4 domain of Bcl-XL, in contrast to that of Bcl-2, directly binds to and inhibits VDAC1 activity as a Ca^{2+}-transport system at the OMM. Notably, although both BH4-Bcl-2 and BH4-Bcl-XL protected against a Ca^{2+}-dependent apoptotic stimulus, a peptide corresponding to the N-terminal region of VDAC1 (VDAC1-NP) exclusively alleviated the anti-apoptotic properties of BH4-Bcl-XL but not those of BH4-Bcl-2 (Fig. 4*C*). Conversely, we showed (21) that the anti-apoptotic properties of BH4-Bcl-2 were abrogated by an IP_3R-derived peptide corresponding to the Bcl-2-binding site (IDP), although it was not the case for BH4-Bcl-XL. Collectively, our results implicate a selective function for the BH4 domains of Bcl-2 and Bcl-XL proteins in targeting the main Ca^{2+}-transport systems at the ER/mitochondrial interface. The BH4 domain of Bcl-2 would function as an inhibitor of IP_3R channels, but not of VDAC1, by targeting the central modulatory domain of IP_3Rs, whereas the BH4 domain of Bcl-XL would function as an inhibitor of VDAC1, but not of IP_3R channels, likely by acting at the level of its N-terminal region (see Fig. 5 for a model).

The VDAC1 high conductance channel has previously been implicated as the major Ca^{2+}-transport system mediating Ca^{2+} flux across the OMM (8, 11, 39, 44–46). Ca^{2+} is then further transported from the inter-membrane space into the mitochondrial matrix via the recently identified mitochondrial Ca^{2+} uniporter (47, 48). The expression levels of VDAC1 thereby have a direct impact on the mitochondrial Ca^{2+} uptake.

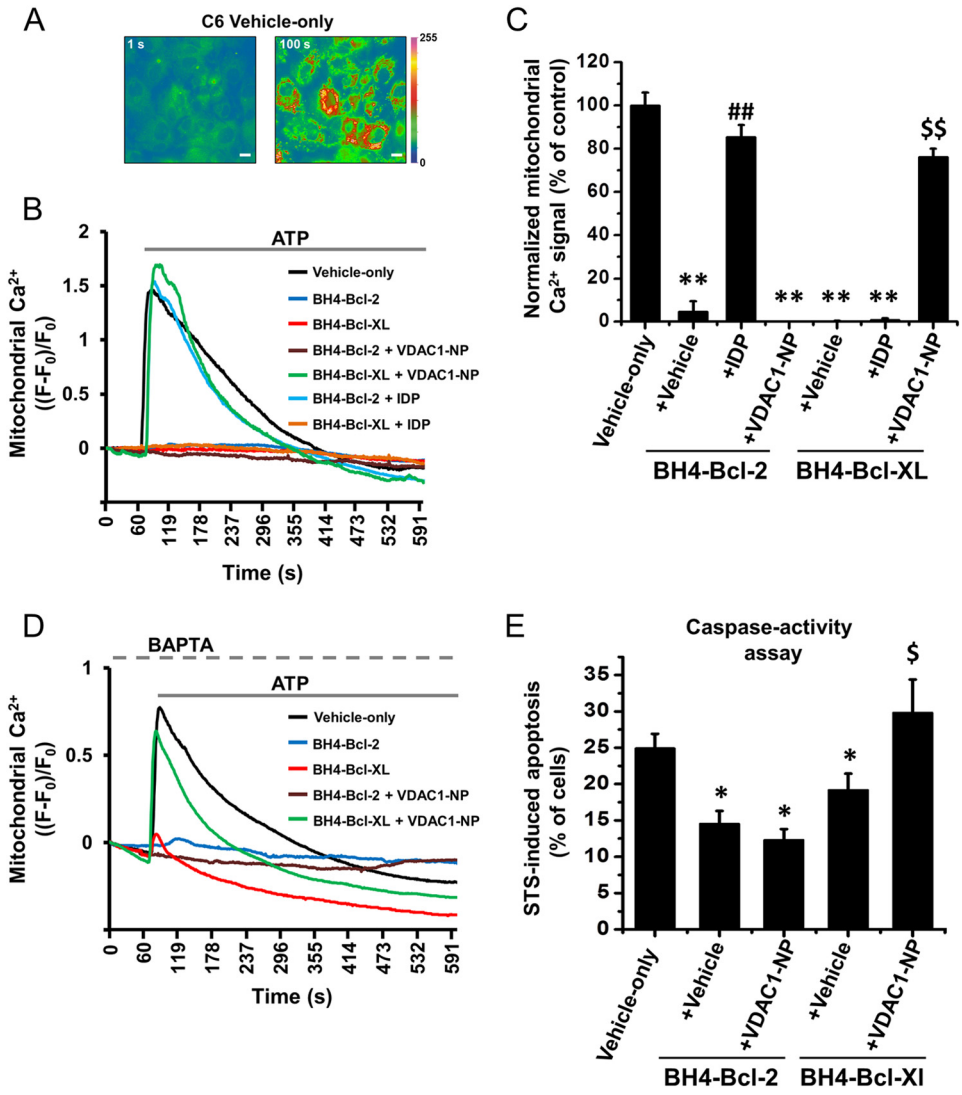

FIGURE 4. **BH4-Bcl-XL, in contrast to BH4-Bcl-2, affects ER-mitochondrial Ca^{2+} transfer and STS-induced apoptosis by specifically acting on VDAC1.** *A,* typical pseudo-colored images resulting from the loading of *in situ* electroporated (0.2% DMSO) C6 glioma cells with Rhod-FF-AM, before (*left panel*; 1 s) and after (*right panel*; 100 s) exposure to ATP (2 μM). ATP was administered at 60 s. *B,* representative mitochondrial Ca^{2+} traces in Rhod-FF-loaded C6 glioma cells challenged with ATP (2μM) after *in situ* electroporation with vehicle only (0.2% DMSO) or the different sets of peptides (20 μM in 0.2% DMSO, see color-coded legend). *C,* quantitative analysis of the area under the curve obtained from five independent experiments as in *A*. Data were normalized to the control condition (vehicle-only), which was set as 100%, and are plotted as means ± S.E. *D,* representative mitochondrial Ca^{2+} traces obtained from C6 glioma cells treated as in *A* but in the absence of extracellular Ca^{2+} (BAPTA 3 mM). *E,* quantification of the percentage of C6 glioma cells stained positive for active caspases in response to STS (2 μM, 6 h) and in the presence (*in situ* electroporation) of vehicle-only (0.2% DMSO) or of the different sets of peptides (20 μM in 0.2% DMSO, see color-coded legend). Data were plotted as means ± S.E. *C* and *E,* * specifies the statistically significant difference between each given condition and the vehicle, and # and $ specify the statistical significance in comparison with, respectively, BH4-Bcl-2 or BH4-Bcl-XL electroporation. Statistically significant differences were considered at $p < 0.05$ (*single symbols*), $p < 0.01$ (*double symbols*).

VDAC1 overexpression enhances mitochondrial Ca^{2+} uptake, whereas VDAC1 silencing impairs mitochondrial Ca^{2+} uptake (11, 39). Here, we support these findings using VDAC1$^{-/-}$ MEFs, which displayed a marked reduction in mitochondrial Ca^{2+} uptake in response to ATP (Fig. 1, *A–C*). Consistent with this, ATP-induced Ca^{2+} signals in the cytosol were higher in VDAC1$^{-/-}$ MEFs (Fig. 1, *D* and *E*). These data are also fully in line with previous work showing that VDAC1 knockdown mainly impacts mitochondrial Ca^{2+} transfer without affecting the ER Ca^{2+}-release kinetics (11). Hence, in intact cells, it is anticipated that there is a "quasi-synaptic" Ca^{2+} transfer between ER and mitochondria, involving both IP_3Rs at the ER and VDAC1 in the OMM (49, 50). In permeabilized cells, microsomal preparations, or isolated mitochondria, these ER/mitochondrial junctions might be lost (39, 51, 52). In these experimental conditions, mitochondrial Ca^{2+} uptake might be granted by the activity of Ca^{2+}-transport systems other than VDAC1 and located outside the MAMs (*e.g.* the other VDAC isoforms that have been proven to be able to permeate Ca^{2+} (11)). In particular, the role that VDAC1 plays in mitochondrial Ca^{2+} transfer makes it the prime route for conveying pro-apoptotic Ca^{2+} signals to the mitochondria. Silencing of VDAC1, but not of VDAC2 or VDAC3, suppressed H_2O_2-induced mitochondrial Ca^{2+} uptake and rendered cells more resistant to apoptosis triggered by H_2O_2 or ceramide, also acting via Ca^{2+} (11, 39). In addition, siRNA-mediated down-regulation of VDAC1 prevented cell death by cisplatin (53) and attenuated endostatin-induced apoptosis (54).This functional role of

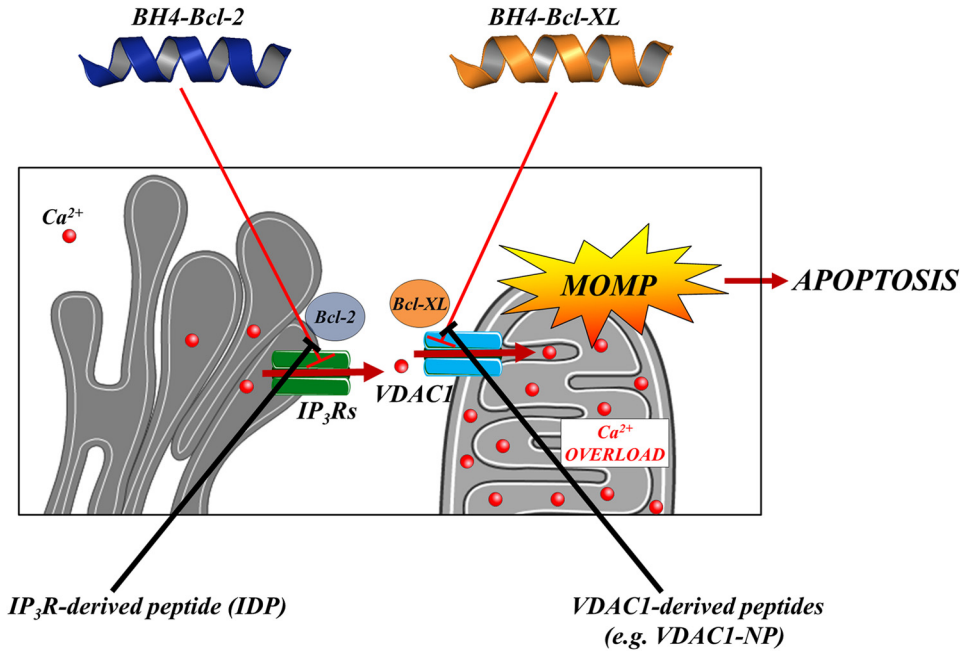

FIGURE 5. **Proposed role of Bcl-2 and Bcl-XL BH4 domains at the ER-mitochondrial interface.** An excessive Ca^{2+} transfer from ER to the mitochondria, via the IP_3R-VDAC1 contact site, promotes MOMP and consequently apoptosis. According to our previous results (21), Bcl-2 protects against Ca^{2+}-mediated apoptosis mainly by using its BH4 domain to interact and inhibit IP_3Rs at the ER membranes. The results of this study indicate that BH4-Bcl-XL protection is dependent on its inhibition, downstream from the same signaling pathway, of the Ca^{2+}-flux properties of mitochondrial outer membrane-located VDAC1 channel likely by interacting with its N-terminal domain. Therefore, IP_3R-derived peptides and VDAC1-derived peptides are unique tools for selective BH4 domain-based antagonism of Bcl-2 and Bcl-XL, respectively.

VDAC1 was also supported by molecular data showing that it was mainly VDAC1 that formed a complex with IP_3R channels (9). In our hands, VDAC1-deficient cells were more resistant than their WT counterparts to STS (Fig. 1*F*), an apoptotic stimulus known to act via intracellular Ca^{2+} mobilization (38). These data validate the concept that VDAC1 critically contributes to mitochondrial Ca^{2+} overload under apoptotic conditions.

Bcl-2 and Bcl-XL are assumed to counteract apoptosis, in part by limiting VDAC1-mediated Ca^{2+} flux into the mitochondria (55). In this paradigm, both proteins are able to bind VDAC1, with only minimal differences in their binding affinities (Fig. 2, *B* and *C*) (26), and to inhibit VDAC1 activity (25–27). The impact of Bcl-2 and Bcl-Xl on the ER-mitochondrial Ca^{2+} fluxes is further supported by their presence in the MAM fraction together with VDAC1 and IP_3Rs (Fig. 2*A*) (9, 40). In this respect, this study is, to the best of our knowledge, the first to prove Bcl-XL's presence at the interface between the two organelles.

Bcl-2 and Bcl-XL directly affect VDAC1 activity presumably by binding different regions of the protein, *e.g.* the N-terminal domain, some of the cytosol-facing loops (namely LP1, LP2, and LP4) (26–28, 56), or part of VDAC1 transmembrane β-barrels (β18 and β19) (57). For the interaction sites on Bcl-2 and Bcl-XL, a prominent role for their BH4 domains was proposed (25), becauseVDAC1-mediated mitochondrial swelling could be alleviated by the presence of either the BH4-Bcl-2 or the BH4-Bcl-XL peptide. Although these measurements were not geared toward the Ca^{2+}-flux properties of VDAC1, careful analysis of the results nevertheless indicated that BH4-Bcl-XL is much more effective in suppressing VDAC1 activity than BH4-Bcl-2. Our results show for the first time that VDAC1 is BH4-Bcl-XL's preferential target at the molecular and functional level, as we observed an exclusive ability of the BH4-Bcl-XL peptide to bind VDAC1 (Fig. 2*D*) and to reduce its conductance (Fig. 3, *A–D*).

The inability of BH4-Bcl-2 peptides to affect channel conductance, further suggests that the effect of BH4-Bcl-XL is due to a specific interaction with VDAC1 and not to a mere penetration into the VDAC1 pore thereby blocking ion movement. Remarkably, BH4-Bcl-XL's effect on VDAC1 activity is more pronounced at the low voltage differences (±10 mV), resembling the physiological OMM potentials (58, 59). In addition to this, the inherent ability of BH4-Bcl-XL to accumulate in mitochondrial membranes (24) correlates with its role on VDAC1. Nonetheless, it still remains to be determined whether BH4-Bcl-2 possesses a similar ability to accumulate in mitochondria because it shares with BH4-Bcl-XL common molecular determinants (positively charged residues and α-helical properties) for mitochondrial targeting (Arg-6/Lys-16/Lys-20 on BH4-Bcl-XL; Arg-12/Lys-22/Arg-26 on BH4-Bcl-2).

Additional experiments revealed that both BH4-Bcl-2 and BH4-Bcl-XL suppress the ATP-induced and VDAC1-mediated Ca^{2+} uptake in the mitochondria, protecting the cells against apoptosis (Fig. 4, *A–E*) (21). However, only the BH4-Bcl-XL effect is alleviated by co-incubation with VDAC1-NP. This indicates that the protective effect of BH4-Bcl-XL is mediated through inhibition of VDAC1 likely by acting at the level of the N terminus. These data are in good agreement with previous reports showing that Bcl-XL binding to VDAC1 was abrogated in VDAC1 lacking its N terminus (26). However, further experiments are required to unequivocally determine the relative

importance of the N-terminal domains of VDAC1 and of Bcl-XL (*i.e.* the BH4 domain) in the context of their full-length protein/protein interaction.

Interestingly, the targeting of VDAC1 by BH4-Bcl-XL may not be limited to mitochondrial VDAC1 but likely can be extended to plasmalemmal VDAC1 (pl-VDAC1) (60). pl-VDAC1 seems to open in response to hypotonic conditions, whereas a peptide covering the BH4 domain of Bcl-XL keeps it closed. In the latter study, a mechanism involving the N terminus of pl-VDAC1 was also suggested. Furthermore, additional sites, besides the N terminus of the mitochondrial VDAC1, have been reported to account for the interaction between the full-length Bcl-2/Bcl-XL and mitochondrial VDAC1 (25, 26, 56, 61), emphasizing the possibility that distinct protein domains may underlie the formation of VDAC1·Bcl-XL *versus* VDAC1·Bcl-2 protein complexes.

Finally, in contrast to our findings and those of others (26, 62), recent reports indicated that anti-apoptotic Bcl-XL and Mcl-1 are both able to enhance VDAC1-mediated Ca^{2+} transfer into the mitochondria under some conditions (51, 63). Indeed, their overexpression enhanced while their deficiency suppressed mitochondrial Ca^{2+} uptake (51, 63). These effects were not observed in VDAC1-deficient cells and were counteracted by N-terminal VDAC1-derived peptides (51, 63). These opposite results might be due to differences in cellular models (*e.g.* the use of Bcl-XL knock-out MEF cells in Ref. 47) and in experimental approaches. In the latter instance, we could include the following: 1) the use of intact cells (this study) *versus* permeabilized cells (47); 2) the use of protein domains like the BH4 domain (this study) *versus* full-length proteins (47); and 3) the use of short term methods like electroporation (this study) *versus* long term methods like knock-out and stable overexpression (47). It is of note that in permeabilized cell systems the majority of the mitochondrial Ca^{2+} uptake from the external solution will occur via uptake mechanisms (like VDAC1) spread across the MOM. In contrast, in intact cells exposed to agonists the majority of the mitochondrial Ca^{2+} uptake likely will occur by VDAC1 located at the MAMs. It is therefore possible that regulation of VDAC1 by associated proteins like Bcl-XL in the "bulk" of the MOM is different from the regulation of VDAC1 at the MAMs. Additionally, these apparently conflicting results may reflect the "dual" and opposing role of VDAC1 in cell death and mitochondrial bioenergetics (64–66). Indeed, beyond VDAC1's role in mitochondrial Ca^{2+} overload and apoptosis, VDAC1 also has an essential function for the survival of cells by fine-tuning the activity of the Ca^{2+}-dependent Krebs cycle enzymes as well as by mediating the exchange of mitochondrial metabolites and ATP. Hence, Bcl-XL-enhancing ER-mitochondrial Ca^{2+} cross-talk would correlate with Bcl-XL driving basal mitochondrial bio-energetics by sensitizing IP_3Rs (19, 67) and/or enhancing VDAC1 activity (51, 68–70), although in other conditions it could suppress the excessive and pro-apoptotic flux of Ca^{2+} into mitochondria by dampening VDAC1 activity. In this complex scenario, it will be interesting to decipher the functional switch of VDAC1 from a pro-survival to a lethal Ca^{2+} gate, which may also involve post-translational regulation of VDAC1 (71), Bcl-XL (72), and/or a simultaneous role of other VDAC1-interacting molecules. Pertinently, VDAC1-binding sites for ATP and NADH (73–75) or for hexokinase-II (28, 76), a key enzyme in cell metabolism (77), could partially overlap with the BH4-Bcl-XL-binding surface and therefore potentially compete with Bcl-XL for differentially regulating VDAC1 activity.

In conclusion, this study is the first to reveal a distinct function for the BH4 domain of Bcl-XL *versus* that of Bcl-2 at the level of VDAC1. The results suggest that Bcl-XL at the MAMs is able to regulate apoptosis by modulating Ca^{2+} uptake into the mitochondria and rendering cells more resistant to increased Ca^{2+} release from the ER.

Acknowledgments—We thank Marina Crabbe, Anja Florizoone, Kirsten Welkenhuyzen (Laboratory of Molecular and Cellular Signaling), and Sofie Van Eygen (Laboratory of Cell Death Research and Therapy) for excellent technical help. We are also grateful to Dr. W. J. Craigen (Baylor College of Medicine, Houston, TX) for providing the WT and VDAC1$^{-/-}$ MEFs.

REFERENCES

1. Rizzuto, R., De Stefani, D., Raffaello, A., and Mammucari, C. (2012) Mitochondria as sensors and regulators of calcium signalling. *Nat. Rev. Mol. Cell Biol.* **13,** 566–578
2. Giorgi, C., De Stefani, D., Bononi, A., Rizzuto, R., and Pinton, P. (2009) Structural and functional link between the mitochondrial network and the endoplasmic reticulum. *Int. J. Biochem. Cell Biol.* **41,** 1817–1827
3. Decuypere, J. P., Monaco, G., Bultynck, G., Missiaen, L., De Smedt, H., and Parys, J. B. (2011) The IP_3 receptor-mitochondria connection in apoptosis and autophagy. *Biochim. Biophys. Acta* **1813,** 1003–1013
4. Patergnani, S., Suski, J. M., Agnoletto, C., Bononi, A., Bonora, M., De Marchi, E., Giorgi, C., Marchi, S., Missiroli, S., Poletti, F., Rimessi, A., Duszynski, J., Wieckowski, M. R., and Pinton, P. (2011) Calcium signaling around Mitochondria Associated Membranes (MAMs). *Cell Commun. Signal.* **9,** 19
5. Csordás, G., Renken, C., Várnai, P., Walter, L., Weaver, D., Buttle, K. F., Balla, T., Mannella, C. A., and Hajnóczky, G. (2006) Structural and functional features and significance of the physical linkage between ER and mitochondria. *J. Cell Biol.* **174,** 915–921
6. Naon, D., and Scorrano, L. (2014) At the right distance: ER-mitochondria juxtaposition in cell life and death. *Biochim. Biophys. Acta* **1843,** 2184–2194
7. Gunter, T. E., Buntinas, L., Sparagna, G. C., and Gunter, K. K. (1998) The Ca^{2+} transport mechanisms of mitochondria and Ca^{2+} uptake from physiological-type Ca^{2+} transients. *Biochim. Biophys. Acta* **1366,** 5–15
8. Gincel, D., Zaid, H., and Shoshan-Barmatz, V. (2001) Calcium binding and translocation by the voltage-dependent anion channel: a possible regulatory mechanism in mitochondrial function. *Biochem. J.* **358,** 147–155
9. Szabadkai, G., Bianchi, K., Várnai, P., De Stefani, D., Wieckowski, M. R., Cavagna, D., Nagy, A. I., Balla, T., and Rizzuto, R. (2006) Chaperone-mediated coupling of endoplasmic reticulum and mitochondrial Ca^{2+} channels. *J. Cell Biol.* **175,** 901–911
10. Raturi, A., and Simmen, T. (2013) Where the endoplasmic reticulum and the mitochondrion tie the knot: the mitochondria-associated membrane (MAM). *Biochim. Biophys. Acta* **1833,** 213–224
11. De Stefani, D., Bononi, A., Romagnoli, A., Messina, A., De Pinto, V., Pinton, P., and Rizzuto, R. (2012) VDAC1 selectively transfers apoptotic Ca^{2+} signals to mitochondria. *Cell Death Differ.* **19,** 267–273
12. Shoshan-Barmatz, V., and Golan, M. (2012) Mitochondrial VDAC1: function in cell life and death and a target for cancer therapy. *Curr. Med. Chem.* **19,** 714–735
13. Ivanova, H., Vervliet, T., Missiaen, L., Parys, J. B., De Smedt, H., and Bultynck, G. (2014) Inositol 1,4,5-trisphosphate receptor-isoform diversity in cell death and survival. *Biochim. Biophys. Acta* **1843,** 2164–2183

14. Monaco, G., Vervliet, T., Akl, H., and Bultynck, G. (2013) The selective BH4 domain biology of Bcl-2-family members: IP_3Rs and beyond. *Cell. Mol. Life Sci.* **70,** 1171–1183
15. Eckenrode, E. F., Yang, J., Velmurugan, G. V., Foskett, J. K., and White, C. (2010) Apoptosis protection by Mcl-1 and Bcl-2 modulation of inositol 1,4,5-trisphosphate receptor-dependent Ca2+ signaling. *J. Biol. Chem.* **285,** 13678–13684
16. Shoshan-Barmatz, V., Keinan, N., and Zaid, H. (2008) Uncovering the role of VDAC in the regulation of cell life and death. *J. Bioenerg. Biomembr.* **40,** 183–191
17. Distelhorst, C. W., and Bootman, M. D. (2011) Bcl-2 interaction with the inositol 1,4,5-trisphosphate receptor: role in Ca^{2+} signaling and disease. *Cell Calcium* **50,** 234–241
18. Chen, R., Valencia, I., Zhong, F., McColl, K. S., Roderick, H. L., Bootman, M. D., Berridge, M. J., Conway, S. J., Holmes, A. B., Mignery, G. A., Velez, P., and Distelhorst, C. W. (2004) Bcl-2 functionally interacts with inositol 1,4,5-trisphosphate receptors to regulate calcium release from the ER in response to inositol 1,4,5-trisphosphate. *J. Cell Biol.* **166,** 193–203
19. White, C., Li, C., Yang, J., Petrenko, N. B., Madesh, M., Thompson, C. B., and Foskett, J. K. (2005) The endoplasmic reticulum gateway to apoptosis by Bcl-XL modulation of the $InsP_3R$. *Nat. Cell Biol.* **7,** 1021–1028
20. Monaco, G., Beckers, M., Ivanova, H., Missiaen, L., Parys, J. B., De Smedt, H., and Bultynck, G. (2012) Profiling of the Bcl-2/Bcl-Xl-binding sites on type 1 IP_3 receptor. *Biochem. Biophys. Res. Commun.* **428,** 31–35
21. Monaco, G., Decrock, E., Akl, H., Ponsaerts, R., Vervliet, T., Luyten, T., De Maeyer, M., Missiaen, L., Distelhorst, C. W., De Smedt, H., Parys, J. B., Leybaert, L., and Bultynck, G. (2012) Selective regulation of IP_3-receptor-mediated Ca^{2+} signaling and apoptosis by the BH4 domain of Bcl-2 versus Bcl-Xl. *Cell Death Differ.* **19,** 295–309
22. Putt, K. S., Chen, G. W., Pearson, J. M., Sandhorst, J. S., Hoagland, M. S., Kwon, J. T., Hwang, S. K., Jin, H., Churchwell, M. I., Cho, M. H., Doerge, D. R., Helferich, W. G., and Hergenrother, P. J. (2006) Small-molecule activation of procaspase-3 to caspase-3 as a personalized anticancer strategy. *Nat. Chem. Biol.* **2,** 543–550
23. Kaufmann, T., Schlipf, S., Sanz, J., Neubert, K., Stein, R., and Borner, C. (2003) Characterization of the signal that directs Bcl-xL, but not Bcl-2, to the mitochondrial outer membrane. *J. Cell Biol.* **160,** 53–64
24. McNally, M. A., Soane, L., Roelofs, B. A., Hartman, A. L., and Hardwick, J. M. (2013) The N-terminal helix of Bcl-xL targets mitochondria. *Mitochondrion* **13,** 119–124
25. Shimizu, S., Konishi, A., Kodama, T., and Tsujimoto, Y. (2000) BH4 domain of antiapoptotic Bcl-2 family members closes voltage-dependent anion channel and inhibits apoptotic mitochondrial changes and cell death. *Proc. Natl. Acad. Sci. U.S.A.* **97,** 3100–3105
26. Arbel, N., Ben-Hail, D., and Shoshan-Barmatz, V. (2012) Mediation of the antiapoptotic activity of Bcl-xL protein upon interaction with VDAC1 protein. *J. Biol. Chem.* **287,** 23152–23161
27. Arbel, N., and Shoshan-Barmatz, V. (2010) Voltage-dependent anion channel 1-based peptides interact with Bcl-2 to prevent antiapoptotic activity. *J. Biol. Chem.* **285,** 6053–6062
28. Abu-Hamad, S., Arbel, N., Calo, D., Arzoine, L., Israelson, A., Keinan, N., Ben-Romano, R., Friedman, O., and Shoshan-Barmatz, V. (2009) The VDAC1 N-terminus is essential both for apoptosis and the protective effect of anti-apoptotic proteins. *J. Cell Sci.* **122,** 1906–1916
29. Mertins, B., Psakis, G., Grosse, W., Back, K. C., Salisowski, A., Reiss, P., Koert, U., and Essen, L. O. (2012) Flexibility of the N-terminal mVDAC1 segment controls the channel's gating behavior. *PLoS One* **7,** e47938
30. Zachariae, U., Schneider, R., Briones, R., Gattin, Z., Demers, J. P., Giller, K., Maier, E., Zweckstetter, M., Griesinger, C., Becker, S., Benz, R., de Groot, B. L., and Lange, A. (2012) β-Barrel mobility underlies closure of the voltage-dependent anion channel. *Structure* **20,** 1540–1549
31. Sabirov, R. Z., Sheiko, T., Liu, H., Deng, D., Okada, Y., and Craigen, W. J. (2006) Genetic demonstration that the plasma membrane maxianion channel and voltage-dependent anion channels are unrelated proteins. *J. Biol. Chem.* **281,** 1897–1904
32. Bultynck, G., Szlufcik, K., Kasri, N. N., Assefa, Z., Callewaert, G., Missiaen, L., Parys, J. B., and De Smedt, H. (2004) Thimerosal stimulates Ca^{2+} flux through inositol 1,4,5-trisphosphate receptor type 1, but not type 3, via modulation of an isoform-specific Ca^{2+}-dependent intramolecular interaction. *Biochem. J.* **381,** 87–96
33. Wieckowski, M. R., Giorgi, C., Lebiedzinska, M., Duszynski, J., and Pinton, P. (2009) Isolation of mitochondria-associated membranes and mitochondria from animal tissues and cells. *Nat. Protoc.* **4,** 1582–1590
34. Decrock, E., De Bock, M., Wang, N., Bol, M., Gadicherla, A., and Leybaert, L. (2014) in *Calcium Techniques: A Laboratory Manual* (Parys J. B., Bootman M., Yule D. I., and Bultynck G., eds) pp. 93–112, Cold Spring Harbor Laboratory Press, Cold Spring Harbor, NY
35. Decrock, E., De Vuyst, E., Vinken, M., Van Moorhem, M., Vranckx, K., Wang, N., Van Laeken, L., De Bock, M., D'Herde, K., Lai, C. P., Rogiers, V., Evans, W. H., Naus, C. C., and Leybaert, L. (2009) Connexin 43 hemichannels contribute to the propagation of apoptotic cell death in a rat C6 glioma cell model. *Cell Death Differ.* **16,** 151–163
36. Van Moorhem, M., Decrock, E., Coussee, E., Faes, L., De Vuyst, E., Vranckx, K., De Bock, M., Wang, N., D'Herde, K., Lambein, F., Callewaert, G., and Leybaert, L. (2010) L-β-ODAP alters mitochondrial Ca^{2+} handling as an early event in excitotoxicity. *Cell Calcium* **47,** 287–296
37. Berridge, M. J. (1993) Inositol trisphosphate and calcium signalling. *Nature* **361,** 315–325
38. Harr, M. W., and Distelhorst, C. W. (2010) Apoptosis and autophagy: decoding calcium signals that mediate life or death. *Cold Spring Harb. Perspect. Biol.* 2, a005579
39. Rapizzi, E., Pinton, P., Szabadkai, G., Wieckowski, M. R., Vandecasteele, G., Baird, G., Tuft, R. A., Fogarty, K. E., and Rizzuto, R. (2002) Recombinant expression of the voltage-dependent anion channel enhances the transfer of Ca^{2+} microdomains to mitochondria. *J. Cell Biol.* **159,** 613–624
40. Meunier, J., and Hayashi, T. (2010) Sigma-1 receptors regulate Bcl-2 expression by reactive oxygen species-dependent transcriptional regulation of nuclear factor κB. *J. Pharmacol. Exp. Ther.* **332,** 388–397
41. Lewis, A., Hayashi, T., Su, T. P., and Betenbaugh, M. J. (2014) Bcl-2 family in inter-organelle modulation of calcium signaling; roles in bioenergetics and cell survival. *J. Bioenerg. Biomembr.* **46,** 1–15
42. Rong, Y. P., Aromolaran, A. S., Bultynck, G., Zhong, F., Li, X., McColl, K., Matsuyama, S., Herlitze, S., Roderick, H. L., Bootman, M. D., Mignery, G. A., Parys, J. B., De Smedt, H., and Distelhorst, C. W. (2008) Targeting Bcl-2-IP_3 receptor interaction to reverse Bcl-2's inhibition of apoptotic calcium signals. *Mol. Cell* **31,** 255–265
43. Rong, Y. P., Bultynck, G., Aromolaran, A. S., Zhong, F., Parys, J. B., De Smedt, H., Mignery, G. A., Roderick, H. L., Bootman, M. D., and Distelhorst, C. W. (2009) The BH4 domain of Bcl-2 inhibits ER calcium release and apoptosis by binding the regulatory and coupling domain of the IP_3 receptor. *Proc. Natl. Acad. Sci. U.S.A.* **106,** 14397–14402
44. Deniaud, A., Rossi, C., Berquand, A., Homand, J., Campagna, S., Knoll, W., Brenner, C., and Chopineau, J. (2007) Voltage-dependent anion channel transports calcium ions through biomimetic membranes. *Langmuir* **23,** 3898–3905
45. Liu, Y., Gao, L., Xue, Q., Li, Z., Wang, L., Chen, R., Liu, M., Wen, Y., Guan, M., Li, Y., and Wang, S. (2011) Voltage-dependent anion channel involved in the mitochondrial calcium cycle of cell lines carrying the mitochondrial DNA A4263G mutation. *Biochem. Biophys. Res. Commun.* **404,** 364–369
46. Tan, W., and Colombini, M. (2007) VDAC closure increases calcium ion flux. *Biochim. Biophys. Acta* **1768,** 2510–2515
47. De Stefani, D., Raffaello, A., Teardo, E., Szabò, I., and Rizzuto, R. (2011) A forty-kilodalton protein of the inner membrane is the mitochondrial calcium uniporter. *Nature* **476,** 336–340
48. Baughman, J. M., Perocchi, F., Girgis, H. S., Plovanich, M., Belcher-Timme, C. A., Sancak, Y., Bao, X. R., Strittmatter, L., Goldberger, O., Bogorad, R. L., Koteliansky, V., and Mootha, V. K. (2011) Integrative genomics identifies MCU as an essential component of the mitochondrial calcium uniporter. *Nature* **476,** 341–345
49. Csordás, G., Thomas, A. P., and Hajnóczky, G. (1999) Quasi-synaptic calcium signal transmission between endoplasmic reticulum and mitochondria. *EMBO J.* **18,** 96–108
50. Shoshan-Barmatz, V., Zalk, R., Gincel, D., and Vardi, N. (2004) Subcellular localization of VDAC in mitochondria and ER in the cerebellum. *Biochim. Biophys. Acta* **1657,** 105–114

51. Huang, H., Hu, X., Eno, C. O., Zhao, G., Li, C., and White, C. (2013) An interaction between Bcl-xL and the voltage-dependent anion channel (VDAC) promotes mitochondrial Ca^{2+} uptake. *J. Biol. Chem.* **288,** 19870–19881
52. Baines, C. P., Kaiser, R. A., Sheiko, T., Craigen, W. J., and Molkentin, J. D. (2007) Voltage-dependent anion channels are dispensable for mitochondrial-dependent cell death. *Nat. Cell Biol.* **9,** 550–555
53. Tajeddine, N., Galluzzi, L., Kepp, O., Hangen, E., Morselli, E., Senovilla, L., Araujo, N., Pinna, G., Larochette, N., Zamzami, N., Modjtahedi, N., Harel-Bellan, A., and Kroemer, G. (2008) Hierarchical involvement of Bak, VDAC1 and Bax in cisplatin-induced cell death. *Oncogene* **27,** 4221–4232
54. Yuan, S., Fu, Y., Wang, X., Shi, H., Huang, Y., Song, X., Li, L., Song, N., and Luo, Y. (2008) Voltage-dependent anion channel 1 is involved in endostatin-induced endothelial cell apoptosis. *FASEB J.* **22,** 2809–2820
55. Pinton, P., Giorgi, C., Siviero, R., Zecchini, E., and Rizzuto, R. (2008) Calcium and apoptosis: ER-mitochondria Ca^{2+} transfer in the control of apoptosis. *Oncogene* **27,** 6407–6418
56. Shi, Y., Chen, J., Weng, C., Chen, R., Zheng, Y., Chen, Q., and Tang, H. (2003) Identification of the protein-protein contact site and interaction mode of human VDAC1 with Bcl-2 family proteins. *Biochem. Biophys. Res. Commun.* **305,** 989–996
57. Hiller, S., Garces, R. G., Malia, T. J., Orekhov, V. Y., Colombini, M., and Wagner, G. (2008) Solution structure of the integral human membrane protein VDAC-1 in detergent micelles. *Science* **321,** 1206–1210
58. Lemeshko, V. V. (2006) Theoretical evaluation of a possible nature of the outer membrane potential of mitochondria. *Eur. Biophys. J.* **36,** 57–66
59. Porcelli, A. M., Ghelli, A., Zanna, C., Pinton, P., Rizzuto, R., and Rugolo, M. (2005) pH difference across the outer mitochondrial membrane measured with a green fluorescent protein mutant. *Biochem. Biophys. Res. Commun.* **326,** 799–804
60. Thinnes, F. P. (2012) To the knowledge of the 20GYGFG24 sequence stretch of type-1 VDAC: to understand why BCl-XL B4 domain peptides keep HeLa cells closed in hypotonic surroundings. *Mol. Genet. Metab.* **106,** 253–254
61. Malia, T. J., and Wagner, G. (2007) NMR structural investigation of the mitochondrial outer membrane protein VDAC and its interaction with antiapoptotic Bcl-xL. *Biochemistry* **46,** 514–525
62. Tornero, D., Posadas, I., and Ceña, V. (2011) Bcl-xL blocks a mitochondrial inner membrane channel and prevents Ca^{2+} overload-mediated cell death. *PLoS One* **6,** e20423
63. Huang, H., Shah, K., Bradbury, N. A., Li, C., and White, C. (2014) Mcl-1 promotes lung cancer cell migration by directly interacting with VDAC to increase mitochondrial Ca^{2+} uptake and reactive oxygen species generation. *Cell Death Dis.* **5,** e1482
64. Michels, J., Kepp, O., Senovilla, L., Lissa, D., Castedo, M., Kroemer, G., and Galluzzi, L. (2013) Functions of BCL-XL at the interface between cell death and metabolism. *Int. J. Cell Biol.* 2013, 705294
65. Lemasters, J. J., and Holmuhamedov, E. (2006) Voltage-dependent anion channel (VDAC) as mitochondrial governator–thinking outside the box. *Biochim. Biophys. Acta* **1762,** 181–190
66. Shoshan-Barmatz, V., De Pinto, V., Zweckstetter, M., Raviv, Z., Keinan, N., and Arbel, N. (2010) VDAC, a multi-functional mitochondrial protein regulating cell life and death. *Mol. Aspects Med.* **31,** 227–285
67. Eno, C. O., Eckenrode, E. F., Olberding, K. E., Zhao, G., White, C., and Li, C. (2012) Distinct roles of mitochondria- and ER-localized Bcl-xL in apoptosis resistance and Ca^{2+} homeostasis. *Mol. Biol. Cell* **23,** 2605–2618
68. Vander Heiden, M. G., Chandel, N. S., Schumacker, P. T., and Thompson, C. B. (1999) Bcl-xL prevents cell death following growth factor withdrawal by facilitating mitochondrial ATP/ADP exchange. *Mol. Cell* **3,** 159–167
69. Vander Heiden, M. G., Li, X. X., Gottleib, E., Hill, R. B., Thompson, C. B., and Colombini, M. (2001) Bcl-xL promotes the open configuration of the voltage-dependent anion channel and metabolite passage through the outer mitochondrial membrane. *J. Biol. Chem.* **276,** 19414–19419
70. Jonas, E. A., Hickman, J. A., Chachar, M., Polster, B. M., Brandt, T. A., Fannjiang, Y., Ivanovska, I., Basañez, G., Kinnally, K. W., Zimmerberg, J., Hardwick, J. M., and Kaczmarek, L. K. (2004) Proapoptotic *N*-truncated BCL-xL protein activates endogenous mitochondrial channels in living synaptic terminals. *Proc. Natl. Acad. Sci. U.S.A.* **101,** 13590–13595
71. Kerner, J., Lee, K., Tandler, B., and Hoppel, C. L. (2012) VDAC proteomics: post-translation modifications. *Biochim. Biophys. Acta* **1818,** 1520-1525
72. Kutuk, O., and Letai, A. (2008) Regulation of Bcl-2 family proteins by posttranslational modifications. *Curr. Mol. Med.* **8,** 102–118
73. Zizi, M., Forte, M., Blachly-Dyson, E., and Colombini, M. (1994) NADH regulates the gating of VDAC, the mitochondrial outer membrane channel. *J. Biol. Chem.* **269,** 1614–1616
74. Yehezkel, G., Hadad, N., Zaid, H., Sivan, S., and Shoshan-Barmatz, V. (2006) Nucleotide-binding sites in the voltage-dependent anion channel: characterization and localization. *J. Biol. Chem.* **281,** 5938–5946
75. Villinger, S., Giller, K., Bayrhuber, M., Lange, A., Griesinger, C., Becker, S., and Zweckstetter, M. (2014) Nucleotide interactions of the human voltage-dependent anion channel. *J. Biol. Chem.* **289,** 13397–13406
76. Arzoine, L., Zilberberg, N., Ben-Romano, R., and Shoshan-Barmatz, V. (2009) Voltage-dependent anion channel 1-based peptides interact with hexokinase to prevent its anti-apoptotic activity. *J. Biol. Chem.* **284,** 3946–3955
77. Pastorino, J. G., and Hoek, J. B. (2003) Hexokinase II: the integration of energy metabolism and control of apoptosis. *Curr. Med. Chem.* **10,** 1535–1551